# C−H Functionalization Reactivity of a Nickel−Imide

Stefan Wiese,[†] Jason L. McAfee,[‡] Dale R. Pahls,[‡] Claire L. McMullin,[‡] Thomas R. Cundari,*,[‡] and Timothy H. Warren*,[†]

[†]Department of Chemistry, Georgetown University, Box 571227-1227, Washington, DC 20057, United States
[‡]Department of Chemistry, Center for Advanced Scientific Computing and Modeling (CASCaM), University of North Texas, Denton, Texas 78203, United States

S *Supporting Information*

ABSTRACT: We report bifunctional reactivity of the β-diketiminato Ni(III)−imide [Me$_3$NN]Ni=NAd (**1**), which undergoes H-atom abstraction (HAA) reactions with benzylic substrates R−H (indane, ethylbenzene, toluene). Nickel−imide **1** competes with the nickel−amide HAA product [Me$_3$NN]Ni−NHAd (**2**) for the resulting hydrocarbyl radical R$^{\bullet}$ to give the nickel−amide [Me$_3$NN]Ni−N(CHMePh)Ad (**3**) (R−H = ethylbenzene) or aminoalkyl tautomer [Me$_3$NN]Ni(η^2-CH(Ph)NHAd) (**4**) (R−H = toluene). A significant amount of functionalized amine R−NHAd is observed in the reaction of **1** with indane along with the dinickel imide {[Me$_3$NN]Ni}$_2$(μ-NAd) (**5**). Kinetic and DFT analyses point to rate-limiting HAA from R−H by **1** to give R$^{\bullet}$, which may add to either imide **1** or amide **2**, each featuring significant N-based radical character. Thus, these studies illustrate a fundamental competition possible in C−H amination systems that proceed via a HAA/radical rebound mechanism.
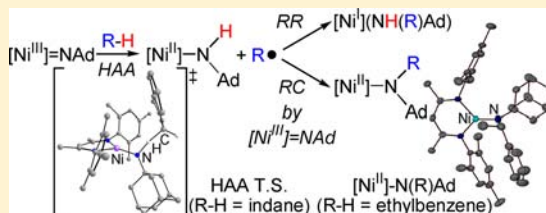
■ INTRODUCTION

Metal−imide (nitrene) intermediates, [M]=NR′,[1] have been implicated in many catalytic C−H amination reactions that allow the atom economical introduction of nitrogen atoms into organic molecules without traditional functional group manipulations.[2] A number of synthetically useful protocols have been developed for both intramolecular and intermolecular C−H amination. Most syntheses that operate through putative nitrene intermediates typically employ electron-withdrawing N-sulfonyl or N-carbamoyl substituents on the nitrene nitrogen to achieve catalytic activity. Dirhodium[3] or ruthenium[4,5] catalysts are common, although catalyst systems utilizing inexpensive first row metals such as Mn,[6] Fe,[7,8] Co,[9] and Cu[10,11] are known. Regardless of the metal, only in a limited number of cases may discrete metal−nitrene intermediates be isolated in these C−H functionalization reactions. For example, Che *et al.* identified (porphyrin)Ru-(=NSO$_2$R)$_2$ species and described their kinetics in the functionalization of benzylic and allylic C−H bonds.[4] Later, Cenini and co-workers isolated the N-aryl analogue (porphyrin)Ru(=NAr^F)$_2$ (Ar^F = 3,5-(CF$_3$)$_2$C$_6$H$_3$) that reacts with C−H bonds of modest strength such as the allylic C−H bond of cyclohexene.[12]

Nickel imides have played key roles in the renaissance of late metal imido chemistry[1] ignited by the 2001 report of the three coordinate terminal imide (dtbpe)Ni=NAr (Ar = 2,6-iPr$_2$C$_6$H$_3$)[13] by Mindiola and Hillhouse, which engages in stoichiometric nitrene group transfer to isocyanides,[14] CO,[14] and ethylene[15] (Figure 1). Formed via η^2-azide adducts (dtbpe)Ni(η^2-N$_3$R),[16] the nickel(II) imides (dtbpe)Ni=NR (R = 1-adamantyl (Ad), 2,4,6-Me$_3$C$_6$H$_2$ (Mes))[16] may be

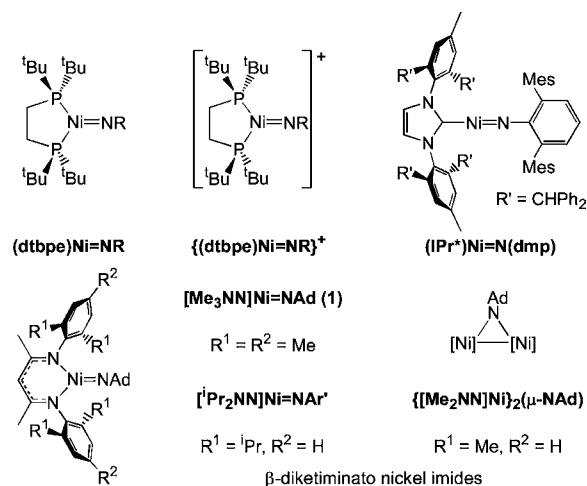**Figure 1.** Nickel imides.

oxidized to their cationic nickel(III) analogues {(dtbpe)Ni=NR}$^+$, which exist in both S = 1/2 (R = Ad and Mes) and S = 3/2 states (R = Ad) (Figure 1).[17] The cationic N-adamantyl species is especially reactive, undergoing facile H-atom abstraction from ether to deliver the cationic nickel(II) amide {(dtbpe)Ni−NHAd}$^+$. Hillhouse also demonstrated that N-heterocyclic carbene ligands may support nickel imides such as the bridging species [(IPr)NiCl]$_2$(μ-NMes) (IPr = 1,3-di(2,6-di-isopropylphenyl)imidazolin-2-ylidene), which catalyzes cata-

lytic nitrene group transfer to isocyanides.[18] Employing an especially bulky N-heterocyclic carbene, Hillhouse observed C−H functionalization reactivity from the two coordinate (IPr*)Ni=N(dmp) in its reaction with ethylene to form CH₂=CHNH(dmp) in addition to nitrene transfer to CO (Figure 1).[19]

Warren and co-workers showed that β-diketiminato ancillary ligands enable the isolation of the dinickel(II) imide {[Me₂NN]Ni}(μ-NAd) as well as the terminal nickel(III) imide [Me₃NN]Ni=NAd from the reaction of N₃Ad with the corresponding nickel(I) precursors [MeₓNN]Ni(2,4-lutidine) (x = 2 or 3) (Figure 1).[20] In addition to clean nitrene transfer to PMe₃ and CO, [Me₃NN]Ni=NAd (**1**) readily abstracts a hydrogen atom from the bis-allylic C−H bond of 1,4-cyclohexadiene (C−H BDE ≈ 77 kcal/mol)[21] to form [Me₃NN]Ni−NHAd (**2**) as well as undergoes radical addition of cobaltocene to the imido N atom resulting in a nickel(II)−amide with a new C−N bond (Scheme 1).[20] DFT calculations

Scheme 1. Reactivity of 1 with Cyclohexadiene and Cp₂Co
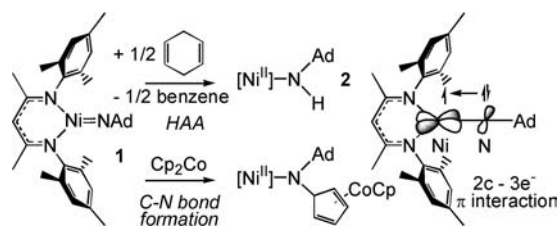
revealed considerable spin density on the imido N atom of **1**, suggesting a description of **1** as a Ni(II)−imidyl species (viz. NR⁻•) that results from the 2-center, 3-electron π-interaction of an imido lone pair with a singly occupied d-orbital on the formally d⁷ Niᴵᴵᴵ center.[20] Such an electronic description also rationalizes the C−C and C−N coupling chemistry at the imido p-aryl position of putative [ⁱPr₂NN]Ni=NAr′ (Ar′ = R₂C₆H₃; R = ⁱPr or Me) intermediates observed in the reaction of {[ⁱPr₂NN]Ni}₂(μ-toluene) with N₃Ar′ reported by Bai and Stephan (Figure 1).[22]

While there are several experimental reports of hydrogen atom abstraction (HAA) reactions of C−H substrates R−H by discrete, mid- to late-first row imido complexes [M]=NR′ (M = Fe,[8,23] Co,[24] Ni,[17,20,25] Cu[11]), considerably more rare is complete functionalization of the C−H bond in R−H to give amines R−NHR′.[8,11,19,26] Cundari and co-workers described computational studies of Fe to Cu nitrene complexes featuring chelating phosphines and β-diketiminate supporting ligands.[27,28] In particular, the thermodynamic favorability of methane C−H amination to give β-diketiminato [M](NH-(Me)R) products increases dramatically as the metal is changed from Fe to Cu in an analogous series of neutral [M]=NR complexes.[28] Consistent with heightened C−H amination reactivity predicted for the copper complexes, the β-diketiminato dicopper nitrene {[Cl₂NN]Cu}₂(μ-NAd) ([Cl₂NN] = 2,4-bis(2,6-dichlorophenylimido)pentyl) participates in the stoichiometric amination of strong C−H bonds such as those in ethylbenzene, toluene, and even cyclohexane, via the putative terminal nitrene [Cl₂NN]Cu=NAd.[11] The β-diketiminato copper(I) complex {[Cl₂NN]Cu}₂(μ-benzene) also catalytically aminates C−H bonds in hydrocarbons (R−H) to give amines (HN(R)Ad) in high yields using N₃Ad as the nitrene transfer reagent (Scheme 2).[11,29]

Scheme 2. Copper Nitrene-Based C−H Amination
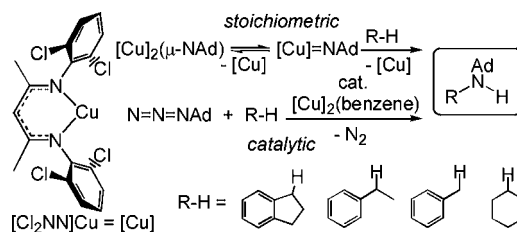
In light of the efficient stoichiometric and catalytic C−H amination by its copper analogue and the aforementioned computational studies of nickel complexes, we reinvestigated the reactivity of [Me₃NN]Ni=NAd (**1**) with benzylic C−H substrates. Specifically, we were interested in the potential to couple previously observed HAA and C−N bond forming reactions (Scheme 1) in a complete C−H functionalization sequence employing a single substrate R−H to give the new amine R−NHAd. A key outcome of the present study, however, reveals that radical addition of R• to the nickel imide [Me₃NN]Ni=NAd (radical capture (RC)) may successfully compete with addition of R• to the nickel-based HAA product [Me₃NN]Ni−NHAd (radical rebound (RR)) that ultimately completes C−H amination to deliver the new amine R−NHAd (Scheme 3).

Scheme 3. Competition between [Ni]−NHAd and [Ni]=NAd for R• Generated by HAA of R−H
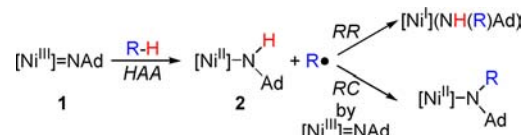
RESULTS

Reaction of [Me₃NN]Ni=NAd (1) with C−H Substrates − Kinetic Analysis. While **1** cleanly reacts with 1,4-cyclohexadiene (C−H BDE ≈ 77 kcal/mol)[21] via HAA to form [Me₃NN]Ni−NHAd (**2**),[20] we find that [Me₃NN]Ni=NAd (**1**) also reacts with hydrocarbon substrates R−H = indane, ethylbenzene, and toluene that possess significantly stronger C−H bonds (C−H BDE = 85, 87, and 90 kcal/mol, respectively).[21] The addition of excess benzylic C−H substrate (200−3000 equiv) to **1** in benzene at 25−65 °C results in the smooth, first-order decay of **1** as monitored by its strong optical band at λ_{max} = 596 nm (Figure 2). Specific variation of the concentration of ethylbenzene indicates first-order dependence in substrate R−H to give the rate expression: rate = k[[Ni]=NAd][R−H]. Comparison of the rates of reaction of **1** with ethylbenzene and ethylbenzene-d_8 leads to a KIE of 4.6(4) at 35 °C, consistent with HAA of R−H by **1** to initially form [Me₃NN]Ni−NHAd (**2**) and R• (Scheme 4). The decreasing second-order rate constants at 35 °C for consumption of **1** by indane ($2.1(2) \times 10^{-4}$ M⁻¹ s⁻¹), ethylbenzene ($2.4(2) \times 10^{-5}$ M⁻¹ s⁻¹), and toluene ($4.5(2) \times 10^{-6}$ M⁻¹ s⁻¹) are also consistent with rate-limiting HAA considering the increasing C−H BDEs of these hydrocarbon substrates. Bearing in mind experimental uncertainties, the free energies of activation also track the increasing C−H BDEs of the C−H substrates and suggest a more ordered transition state (e.g., shorter C···H···N
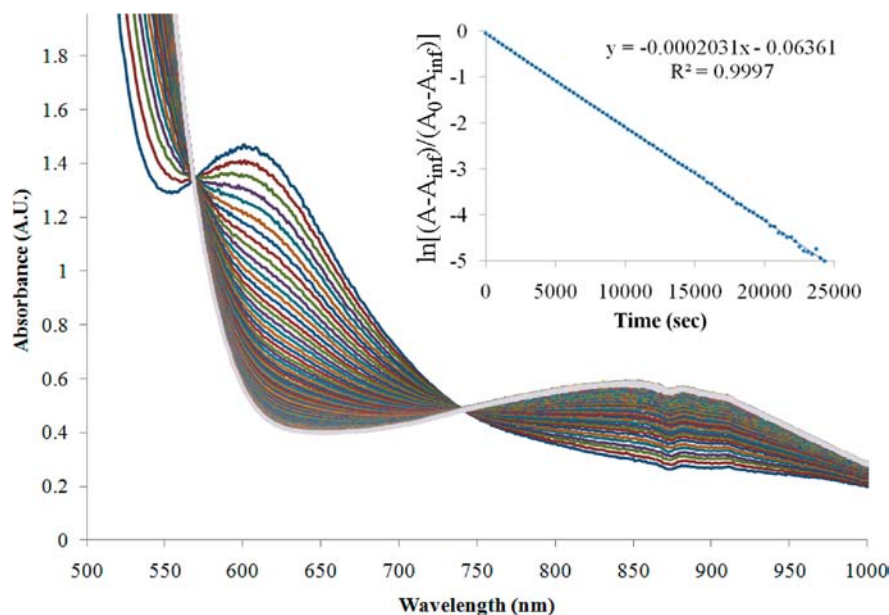
Figure 2. UV−vis trace of reaction of **1** ($[\mathbf{1}]_0$ = 2.32 mM) with 2000 equiv of ethylbenzene in benzene at 45 °C (scan interval = 300 s) monitoring the absorbance of **1** at λ = 596 nm. Inset: Linear plot of $\ln[(A - A_\infty)/(A_0 - A_\infty)]$ versus time.

Scheme 4. Kinetic Data for Reaction of [Me₃NN]Ni=NAd (1) with R−H via Initial HAA

R	C-H BDE (kcal/mol)	$\Delta G^{\ddagger}$(298 K) (kcal/mol)	$\Delta H^{\ddagger}$ (kcal/mol)	$\Delta S^{\ddagger}$ (cal/mol K)
indanyl	85	23.0(15)	13.5(13)	-31(2)
CH(Me)Ph	87	24.2(8)	11.6(7)	-42(2)
CH₂Ph	90	25.1(13)	10.0(10)	-50(3)

Scheme 5. Reactivity of 1 with Ethylbenzene and Toluene to Form 3 and 4

separation and earlier transition state, *vide infra*) as the C−H BDE increases (Scheme 4).

Isolation of New Nickel Products. In contrast to the clean HAA reaction between 0.5 equiv of 1,4-cyclohexadiene and **1** that leads to [Me₃NN]Ni−NHAd (**2**) in >90% spectroscopic yield (Scheme 1), product mixtures that result from the reaction of **1** with benzylic C−H substrates are rather complex and sensitive to reaction conditions. Radicals R• that result from HAA of ethylbenzene, toluene, and indane are better suited for C−N bond formation in comparison to the doubly allylic radical derived from 1,4-cyclohexadiene, which is primed for loss of an H-atom to give benzene. For **1** to convert a substrate R−H to the corresponding C−H amination product R−NHAd, the radical R• must combine with the nickel-based HAA product [Me₃NN]Ni−NHAd (**2**) with high fidelity. A key finding of our studies, however, is that the nickel(III)−imide **1** can successfully compete with nickel(II)−amide **2** for capture of the radical R• (Scheme 3).

The stoichiometric reaction of [Me₃NN]Ni=NAd (**1**) with 100 equiv of ethylbenzene in Et₂O at room temperature (3 h) gave the nickel(II) secondary amido complex [Me₃NN]Ni−N(CHMePh)Ad (**3**) as brown crystals from Et₂O at −35 °C in 49% yield based on total moles of Ni (Scheme 5; max yield = 50%). Similarly, reaction of [Me₃NN]Ni(2-pic) with 1 equiv of N₃Ad in ethylbenzene gave an identical result: a 49% isolated yield of **3**. Thus, the nickel(III)−imide **1** rather efficiently captured the ethylbenzene radical generated via HAA by another equivalent of **1**. The X-ray structure of the three-

coordinate nickel(II)-amide **3** reveals a short Ni−N$_{amido}$ distance of 1.790(5) Å along with relatively short Ni−N$_{\beta\text{-dik}}$ distances of 1.879(4) and 1.876(4) Å (Figure 3). These parameters are comparable to those in the related nickel(II)−amide [Me₃NN]Ni−NAd(η^4-C₅H₅)CoCp (Ni−N$_{amido}$ = 1.812(3) Å, Ni−N$_{\beta\text{-dik}}$ = 1.881(3) and 1.879(3) Å) illustrated in Scheme 1.[20] The two Ni−N$_{amido}$−C angles of 122.5(4)° and 123.7(5)° in **3** along with the sum of the angles about N$_{amido}$ (359.5(4)°) are consistent with a planar, sp²-hybridized N$_{amido}$ donor. We note that the nickel(II)−amide [Me₃NN]Ni−NAd(η^4-C₅H₅)CoCp forms by addition of the cobaltocene radical to **1** to give a new C−N bond (Scheme 1) just as the new nickel(II)−amide **3** forms by capture of an ethylbenzene radical by **1** (Scheme 5).

The stoichiometric reaction of [Me₃NN]Ni=NAd (**1**) with neat toluene at room temperature (3 days) yielded the nickel(II) secondary aminoalkyl complex [Me₃NN]Ni(η^2-CH(Ph)NHAd) (**4**) as brown crystals from Et₂O at −35 °C in 38% yield based on total moles of Ni (Scheme 4; max yield = 50%). The connectivity of **4** was determined by X-ray crystallography and revealed an η^2-aminoalkyl group with a Ni−C bond. Complex **4** likely forms via the tautomerization of [Me₃NN]Ni−N(CH₂Ph)Ad via a β-H elimination/reinsertion sequence after initial capture of a benzyl radical by the imido nitrogen of **1**. The X-ray structure of **3** (Figure 3) reveals a four-coordinate nickel(II)-aminoalkyl species **4** with Ni−C$_{alkyl}$
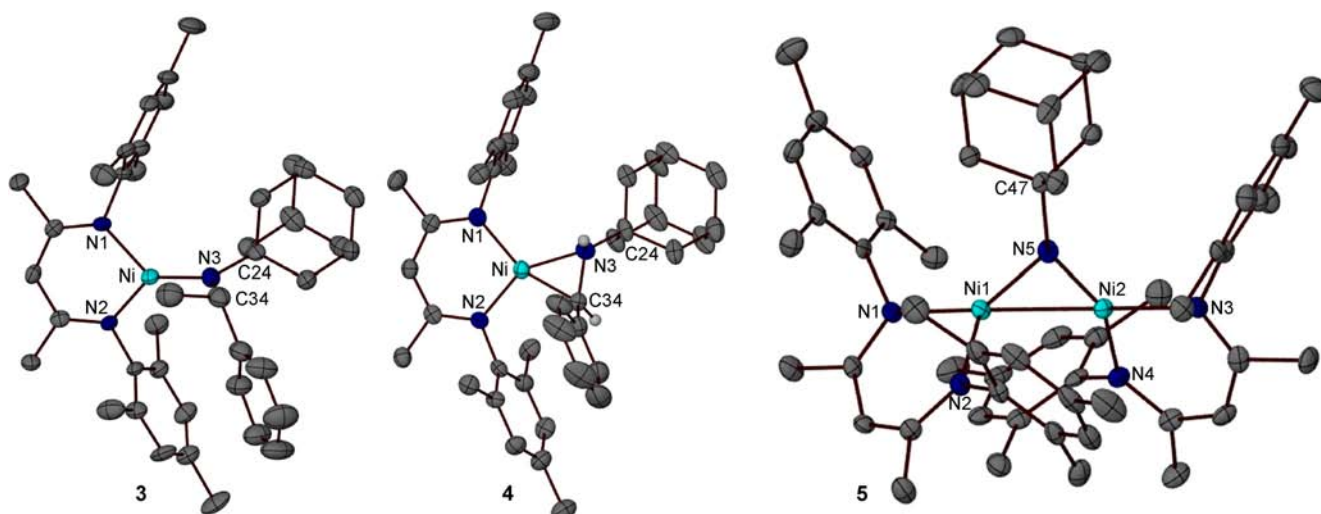
10116

dx.doi.org/10.1021/ja302149k | *J. Am. Chem. Soc.* 2012, 134, 10114−10121

Figure 3. X-ray structures of [Me$_3$NN]Ni−N(CHMePh)Ad (**3**), [Me$_3$NN]Ni(η^2-CH(Ph)NHAd) (**4**), and {[Me$_3$NN]Ni}$_2$(μ-NAd) (**5**).

and Ni−N$_{amine}$ bond distances of 1.897(4) and 1.936(3) Å, respectively, along with a highly acute Ni−C$_{alkyl}$−N$_{alkyl}$ angle of 69.4(3)°. The Ni−N$_{\beta\text{-dik}}$ distances are 1.917(3) and 1.872(3) Å. Such asymmetric Ni−N$_{\beta\text{-dik}}$ bond distances were also observed in the related β-agostic alkyl complex [Me$_2$NN]Ni(η^2-CH$_2$CH$_3$) (1.892(3) and 1.859(3) Å).[30] As in the β-agostic alkyl complex, the elongated Ni−N$_{\beta\text{-dik}}$ distance in **4** is trans to the Ni−C covalent bond.
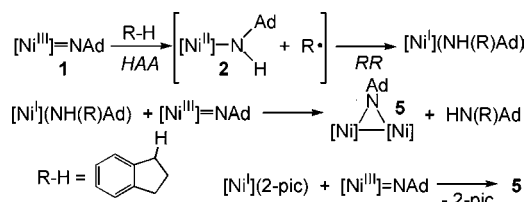
In the stoichiometric reaction of **1** and neat indane (100 equiv) at room temperature (1 day), we did not isolate any product consistent with addition of the indanyl radical to **1**. Rather, we isolated the dinickel imide {[Me$_3$NN]Ni}$_2$(μ-NAd) (**5**) as brown crystals from Et$_2$O at −35 °C in 52% yield (Scheme 6). The X-ray structure of **5** (Figure 3) shows Ni−

Scheme 6. Reactivity of 1 with Indane to Give [Ni]$_2$(μ-NAd) (5)

NAd distances of 1.738(3) and 1.758(3) Å along with a Ni−Ni distance of 2.4872(7) Å. This species is nearly identical in structure to the previously reported {[Me$_2$NN]Ni}$_2$(μ-NAd).[20] These dinickel adamantylimido complexes may be directly compared to their Cu analogue {[Me$_3$NN]Cu}$_2$(μ-NAd),[11] which has Cu−NAd distances of 1.785(6) and 1.821(5) Å along with a much longer Cu···Cu separation of 2.901(2) Å. EPR analysis indicates at least partial dissociation of **5** to [Me$_3$NN]Ni=NAd (g_{iso} = 2.05) and [Me$_3$NN]Ni(solvent) (g_{iso} = 2.21) at room temperature (ca. 1 mM in toluene). Thus, [Ni]$_2$(μ-NR) intermediates may act as a reservoir for terminal [Ni]=NR species.

We propose that the dinickel species {[Me$_3$NN]Ni}$_2$(μ-NAd) (**5**) isolated from the reaction of **1** with indane results from the complexation of [Me$_3$NN]Ni=NAd (**1**) by a Ni(I) species in solution such as [Me$_3$NN]Ni(NH(indanyl)Ad) generated by the complete C−H amination of indane by **1**.

In support of this proposal, addition of the nickel(I) 2-picoline adduct [Me$_3$NN]Ni(2-pic) to **1** allows for the isolation of dinickel imide **5** in 78% yield (Scheme 6). Direct "rebound" of the 1-indanyl radical to **2** is substantiated by the ^{1}H NMR identification of the C−H functionalized organic product NH(1-indanyl)Ad in 33% yield when **1** is allowed to react with 200 equiv of indane in Et$_2$O at room temperature. Separate reactivity studies under analogous conditions show that dinuclear **5** is essentially unreactive toward indane. In light of this observation, the maximum amount of the functionalized amine NH(1-indanyl)Ad to be expected is ca. 50%.

Theory − H-Atom Abstraction by [Me$_3$NN]Ni=NAd (1). We employed theory to examine several details relevant to the hydrocarbon reactivity of **1** and the formation of species **3**−**5**. At the ONIOM(B3LYP:6-311++G(d,p):UFF) level of theory, we calculated the N−H bond dissociation enthalpy in [Me$_3$NN]Ni−NHAd (**2**) to be 85.2 kcal/mol. Comparison against the value of 83.8 kcal/mol calculated for the BDE of a benzylic C−H bond in ethylbenzene supports the contention that [Me$_3$NN]Ni=NAd (**1**) could engage in HAA reactions with related benzylic substrates.
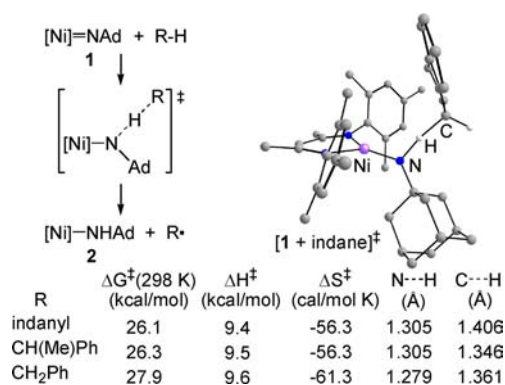
To computationally evaluate the kinetic feasibility of these HAA reactions, we identified S = 1/2 transition states for HAA from indane, ethylbenzene, and toluene by [Me$_3$NN]Ni=NAd (**1**). These transition states are 26.1−27.9 kcal/mol higher in free energy than separated **1** and the corresponding benzylic substrate R−H (Scheme 7). Principally due to a tighter transition state (shorter C···H···N separation, Scheme 7) with increasing substrate C−H bond strength, the calculated $\Delta G^{\ddagger}$ values at 298 K increase with increasing C−H bond strength and track well with the experimentally determined values (Scheme 4). In each HAA transition state, the imido N atom attacks the C−H bond in an "axial" direction relative to the trigonal imide **1**, with the incipient N−H bond roughly positioned as it appears in the product nickel−amide [Me$_3$NN]Ni−NHAd (**2**) (Scheme 7). Comparison of the C···H and N···H distances among the three transition states reveals that the T.S. becomes more ordered (e.g., tighter C···H···N linkage) as the C−H bond strength of the hydrocarbon substrate increases from indane to toluene. Prompted by the S = 1 state identified for [Me$_3$NN]Ni−NHAd (see below), the S = 3/2 transition state for HAA of

Scheme 7. Calculated Activation Parameters for HAA by 1 and Transition State for HAA from Indane

R	$\Delta G^{\ddagger}$(298 K) (kcal/mol)	$\Delta H^{\ddagger}$ (kcal/mol)	$\Delta S^{\ddagger}$ (cal/mol K)	N···H (Å)	C···H (Å)
indanyl	26.1	9.4	-56.3	1.305	1.406
CH(Me)Ph	26.3	9.5	-56.3	1.305	1.346
CH₂Ph	27.9	9.6	-61.3	1.279	1.361

indane was found to be 3.4 kcal/mol higher in free energy than the corresponding $S = 1/2$ transition state.

Theory − Nickel(II)−Amido Complexes. Experimentally, [Me₃NN]Ni−NHAd (**2**) possesses a solution magnetic moment of ca. 1.0 μ_B,[20] suggesting contributions from both singlet and triplet spin states. On the other hand, amide **3** and aminoalkyl **4** have solution moments of 0.0 μ_B. QM/MM calculations on amides **2** and **3** suggest that the triplets are close in energy to the singlet, located 3.2 and 2.3 kcal/mol (free energy) below the singlet in the gas phase, respectively. For Ni(II)−aminoalkyl species **4**, however, calculations place the triplet state significantly higher than the singlet by ca. 9 kcal/mol. Calculations also indicate that the Ni(II)−aminoalkyl **4** is 5.2 kcal/mol lower in free energy than the Ni(II)−amide tautomer [Me₃NN]Ni−N(CH₂Ph)Ad that directly results from capture of the PhCH₂• radical by **1** (Scheme 4). Consistent with experiment, the free energy ordering of the aminoalkyl and amido tautomers from capture of an ethylbenzene radical by **1** is reversed: amide **3** is favored over the tertiary aminoalkyl [Me₃NN]Ni(η²-CMe(Ph)NHAd) by 4.2 kcal/mol.

As summarized in Scheme 8, the addition of a benzylic radical R• derived from indane, ethylbenzene, or toluene to

**Scheme 8. Calculated Thermochemistry for Addition of Benzylic Radicals R• to 1 and 2-S=1**

R•	ΔH	ΔG	ΔH	ΔG (kcal/mol)
indanyl	-41.2	-23.3	-21.0	-3.1
CH(Me)Ph	-40.8	-22.1	-21.2	-2.9
CH₂Ph	-46.0	-29.3	-26.5	-9.5
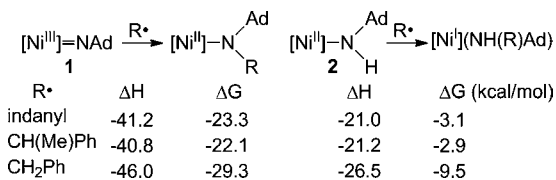
[Me₃NN]Ni═NAd (**1**) is significantly more thermodynamically favored than "rebound" of this radical R• to the metal−amide [Me₃NN]Ni−NHAd (**2**), the initial product of HAA by **1**. Nonetheless, it is not straightforward to computationally predict the outcome of these competing reactions because these radical combination reactions are likely to have low kinetic barriers, especially when considering the triplet state of [Me₃NN]Ni−NHAd (**2-S=1**).

Scheme 8 also indicates that radical capture is thermodynamically favored by an average of ~20 kcal/mol for addition of R• to Ni−imide versus addition of the radical to Ni−amide. The calculated thermodynamics in Scheme 8 are consistent with the hypothesis that radical capture by the Ni−imide **1** may compete with radical rebound to the Ni−amide **2**, especially as

the former may be present in significant concentration in solution. Finally, we note that HAA by [Ni^II]−N(R)Ad is calculated to be significantly endergonic (ΔG's > 17 kcal/mol) for the substrates studied here, implying that the Ni−amides are not expected to compete with Ni−imides for substrate C−H bond activation (Scheme S1).

Both **1** and **2-S=1** possess significant unpaired electron density at the imido or amido N atom (Figures 4 and S15). The
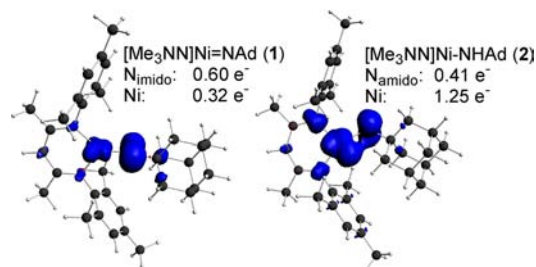
Figure 4. Spin density plots of **1** and **2-S=1** (0.003 isospin value; ADF 2007.1/BP/ZORA/TZ2P(+)).

triplet state of amide [Me₃NN]Ni−NHAd (**2-S=1**) features a "twisted" amido group that is only ca. 30° out of planarity with the β-diketiminate backbone, whereas both the calculated geometry for singlet **2** as well as the X-ray crystal structure of **2** indicate an orthogonal arrangement of the amide relative to the β-diketiminate backbone. A lengthening of the Ni−N_amide distance calculated for triplet **2-S=1** (1.831 Å) relative to singlet **2** (1.786 Å) and that found in its X-ray structure (1.742(4) Å) accompanies this conformational change.

DISCUSSION AND CONCLUSIONS

The relatively high N−H bond strength in [Me₃NN]Ni−NHAd (**2**) facilitates HAA reactions of [Me₃NN]Ni═NAd (**1**) with indane, ethylbenzene, and toluene under mild conditions at rates that decrease with increasing C−H bond strength. A key outcome of this study reveals that the nickel imide **1** can capture the radical R• generated in the HAA reaction of **1** with R−H to provide the diamagnetic nickel amido [Me₃NN]Ni−N(CHMePh)Ad (**3**) and alkylamine [Me₃NN]Ni(η²-CH(Ph)-NHAd) (**4**) products from the reaction of **1** with ethylbenzene and toluene, respectively (Scheme 3). Thus, radical addition to **1** competes with capture of R• by [Me₃NN]Ni−NHAd (**2**) required to complete "insertion" of the NAd group of **1** into the C−H bond of R−H to give coordinated R−NHAd, the amine product of C−H functionalization (Scheme 3).

It is interesting to note that only in the reaction of [Me₃NN]Ni═NAd (**1**) with excess indane (200 equiv in ether) may an appreciable amount of the C−H amination product be observed ((1-indanyl)NHAd, 33% yield). Under analogous conditions with ethylbenzene or toluene, less than <5% of the corresponding functionalized amine R−NHAd is observed. Because there is little calculated energetic difference between the addition of the indanyl or ethylbenzene radical to either **1** or **2** (although addition to **1** is strongly favored), this finding is somewhat striking. Bearing in mind the larger size and greater rigidity of the indanyl radical versus that of the ethylbenzene (and benzyl) radical, it appears that steric accessibility to the nitrogen atom of imide **1** versus amide **2** plays an important role.[31] The longer Ni−N bond in amide **2**, especially in its triplet form (1.831 Å (calc)) as compared to imide **1** (1.662(2) Å (X-ray); 1.670 Å (calc)) should allow

greater access of a more sterically encumbered radical to the nickel-bound amido N atom of **2**. Furthermore, the "twisted" nature of the nickel−amide linkage in **2-S=1** orients N-based spin-density differently from in nickel−imide **1** (Figure 4), perhaps allowing for smoother C−N bond formation with the rigid indanyl radical.

Regarding the role of late transition metal−imides [M]=NR′ in C−H amination, these studies illustrate that more is required for successful C−H amination than simply a strong N−H bond in the corresponding metal−amide [M]−NHR′. While a strong N−H bond certainly provides driving force for HAA from the C−H substrate R−H, it should also thermodynamically favor the addition of the radical R• to the metal−imide [M]=NR′ to give the metal−amide [M]−NRR′, a key outcome observed in this study. Both the amount of unpaired electron density at the N atom in [M]=NR′ and [M]−NHR′ species as well as the relative accessibility of these different types of N atoms are likely important determinants of the site of R• attack.

In this light, the relatively unselective C−H functionalization reactivity of **1** should be contrasted with the highly selective stoichiometric and catalytic C−H amination of benzylic substrates R−H by {[Cl$_2$NN]Cu}$_2$(μ-NAd).[11] Proceeding through the presumed $S = 0$ intermediate [Cl$_2$NN]Cu=NAd, likely present in only a small amount in solution via the dissociation of a [Cl$_2$NN]Cu fragment from {[Cl$_2$NN]Cu}$_2$(μ-NAd) (Scheme 2),[11] a related HAA reaction with R−H would result in the copper(II)−amide [Cl$_2$NN]Cu−NHAd.[32] The copper nitrene possesses significantly more driving force for HAA reflected in the N−H bond dissociation enthalpy of 98.4 kcal/mol calculated for [Cl$_2$NN]Cu−NHAd as compared to 85.2 kcal/mol for [Me$_3$NN]Ni−NHAd (**2**). Comparison of the addition of R• to [Me$_3$NN]Ni−NHAd (**2**) ($\Delta G = -2.9$ to -9.5 kcal/mol; Scheme 8) and [Cl$_2$NN]Cu−NHAd ($\Delta G = -14.7$ to -17.9 kcal/mol; Scheme 9) reveals a notable difference in

Scheme 9. Calculated Thermochemistry for Addition of Benzylic Radicals R• to [Cl$_2$NN]Cu=NAd and [Cl$_2$NN]Cu−NHAd

R•	ΔH	ΔG	ΔH	ΔG (kcal/mol)
indanyl	-66.4	-47.4	-35.1	-17.2
CH(Me)Ph	-63.1	-45.0	-31.3	-14.7
CH$_2$Ph	-67.7	-50.8	-34.5	-17.9

driving force favoring radical addition to the copper(II)−amide that possesses a significant amount of spin density at the amido N atom (0.49 e$^-$).[32] While radical addition of R• to both [Cl$_2$NN]Cu=NAd and [Cl$_2$NN]Cu−NHAd is highly favored thermodynamically (Scheme 9), clean C−H amination with substrates R−H by {[Cl$_2$NN]Cu}$_2$(μ-NAd) may also be promoted by the presumably low concentration of the putative [Cl$_2$NN]Cu=NAd active intermediate generated by dissociation of a [Cl$_2$NN]Cu fragment from {[Cl$_2$NN]Cu}$_2$(μ-NAd) (Scheme 2).

■ EXPERIMENTAL SECTION

General Procedures. All experiments were carried out in a dry nitrogen atmosphere using an MBraun glovebox and/or standard Schlenk techniques. 4A molecular sieves were activated in vacuo at 180 °C for 24 h. Diethyl ether and tetrahydrofuran (THF) were first sparged with nitrogen and then dried by passage through activated

alumina columns. Pentane was first washed with concentrated HNO$_3$/H$_2$SO$_4$ to remove olefins, stored over CaCl$_2$, sparged, and then passed through activated alumina columns. Benzene, toluene, and ethylbenzene were purchased anhydrous and stored over 4A molecular sieves. All deuterated solvents were sparged with nitrogen, dried over activated 4A molecular sieves, and stored under nitrogen. Celite was dried overnight at 200 °C under vacuum. ^{1}H and ^{13}C NMR spectra were recorded on a Varian MR 400 MHz spectrometer (400 and 100.47 MHz, respectively). All NMR spectra were recorded at room temperature unless otherwise noted and were indirectly referenced to residual solvent signals or TMS as internal standards. UV−vis spectra were measured on a Varian Cary 50 or 100 spectrophotometer, using airtight quartz cuvettes with screw-cap tops or Teflon stoppers. Solution EPR spectra were recorded on a JEOL continuous wave spectrometer JES-FA200 equipped with an X-band Gunn oscillator bridge and a cylindrical mode cavity employing a modulation frequency of 100 kHz. GC−MS spectra were recorded on a Varian Saturn 3900, and elemental analyses were performed on a Perkin-Elmer PE2400 microanalyzer at Georgetown. IR measurements were performed on a Perkin-Elmer Spectrum One FT-IR spectrometer. All reagents were obtained commercially unless otherwise noted. [Me$_3$NN]Ni=NAd[20] (**1**) and [Me$_3$NN]Tl[20] were prepared by literature methods. Ethylbenzene-d_{10} was obtained from Cambridge Isotope Laboratories, Inc. This deuterated reagent and other deuterated solvents were degassed with N$_2$ and stored over activated 4A molecular sieves prior to use.

Kinetic Measurements by UV−Vis Spectroscopy. A stock solution containing a known amount of freshly prepared [Me$_3$NN]-Ni=NAd (**1**) (typically 0.063−0.134 g) in benzene was prepared using a 10.0 mL volumetric flask. Aliquots of this solution of **1** were mixed with known amounts of ethylbenzene, toluene, or indane (typically 200−3000 equiv/**1**) and diluted to known concentration using either a 3.0 or a 10.0 mL volumetric flask. Each UV−vis run employed ca. 3 mL of a benzene solution containing **1** and C−H substrate in a thermostatted quartz cell. The loss of **1** was monitored by the gradual decrease its absorbance at $\lambda = 596$ nm. In all measurements, **1** followed first-order decay as evidenced by linear plots of $\ln[(A - A_\infty)/(A_0 - A_\infty)]$ versus time (A = absorbance at $\lambda = 596$ that varies with time; A_∞ = final absorbance at $\lambda = 596$ nm; A_0 = initial absorbance at $\lambda = 596$ nm) typically collected for at least three half-lives ($\ln[(A - A_\infty)/(A_0 - A_\infty)] = -2.08$). Specific experimental details and data analysis for the determination of the kinetic order in ethylbenzene, Eyring analysis for ethylbenzene, toluene, and indane, and the determination of KIE for ethylbenzene may be found in the Supporting Information.

Preparation of Compounds. *[Me$_3$NN]Ni(2-picoline).* To a solution of NiI$_2$ (0.595 g, 1.91 mmol) and 2-picoline (0.177 g, 1.91 mmol) in 5 mL of THF was added [Me$_3$NN]Tl (1.0 g, 1.91 mmol). The reaction mixture was allowed to stir for 1 h before it was filtered through Celite to remove insoluble TlI. To the resulting solution was added 11.0 g of Na/Hg (0.5% Na by weight; 2.39 mmol Na), and the solution was allowed to stir for 1 h before it was decanted from the amalgam and filtered through Celite. The solution was concentrated to dryness, and the remaining solid was crystallized from pentane to afford red crystals at −35 °C in 80% yield (0.718 g, 1.52 mmol). UV−vis (Et$_2$O, 25 °C): $\lambda_{max} = 523$ nm ($\varepsilon = 1400$ M^{-1} cm^{-1}); μ_{eff} (benzene-d_6) = 1.55 μ_B (with a drop of 2-picoline added). EPR (toluene, frozen glass, 77 K): $g_1 = 2.41$, $g_2 = 2.12$, $g_3 = 2.06$ (with a drop of 2-picoline added). Anal. Calcd for C$_{29}$H$_{36}$N$_3$Ni: C, 71.77; H, 7.48; N, 8.66. Found: C, 71.52; H, 7.43; N, 8.33.

[Me$_3$NN]Ni−N(CHMePh)Ad (3). To a chilled solution of [Me$_3$NN]-Ni=NAd (**1**) (0.169 g, 0.312 mmol) in 4 mL of Et$_2$O was added 8 mL of a 50:50 mixture of Et$_2$O/ethylbenzene. The reaction mixture was allowed to stir at room temperature for 3 h during which a color change from green to brown occurred. All volatiles were removed in vacuo, and the remaining solid was taken up in Et$_2$O, passed through Celite, and concentrated to afford brown crystals from Et$_2$O at −35 °C in 49% yield based on moles of Ni (0.098 g, 0.153 mmol; max yield = 50%). ^{1}H NMR (C$_6$D$_6$, 400 MHz, room temperature): δ 7.02 (t, 1H, *p*-Ph−*H*), 6.92 (t, 2H, *m*-Ph−*H*), 6.75 (overlapping s, 4H, *m*-Ar−*H*),

6.13 (d, 2H, *o*-Ph−*H*), 4.71 (s, 1H, backbone C−*H*), 3.06 (d, 3H, NCH*Me*), 2.90 (s, 6H, Ar−C*H*$_3$), 2.87 (s, 6H, Ar−C*H*$_3$), 2.82 (d, 3H, Ad−C*H*$_2$), 2.59 (q, 1H, NC*H*Me), 2.19 (s, 6H, Ar−C*H*$_3$), 1.82 (br, 3H, Ad−C*H*), 1.65 (d, 3H, Ad−C*H*$_2$), 1.51 (s, 6H, Ad−C*H*$_2$), 1.24 (s, 6H, backbone-C*H*$_3$). ^{13}C{^{1}H} NMR (C$_6$D$_6$): δ 156.29, 145.92, 134.04, 133.88, 133.52, 129.58, 129.31, 128.15, 127.33, 125.74, 102.44, 67.85, 65.30, 43.50, 37.25, 30.80, 22.46, 21.14, 19.55. Anal. Calcd for C$_{41}$H$_{53}$N$_3$Ni: C, 76.16; H, 8.26; N, 6.50. Found: C, 76.44; H, 8.26; N, 6.55. [Me$_3$NN]Ni−N(CHMePh)Ad (**3**) may also be directly prepared from [Me$_3$NN]Ni(2-picoline) and N$_3$Ad in the presence of excess ethylbenzene. To a chilled solution of [Me$_3$NN]Ni(2-picoline) (0.240 g, 0.494 mmol) in 4 mL of Et$_2$O and 4 mL of ethylbenzene was added cold a solution of 1-azidoadamantane (0.088 g, 0.494 mmol) in 2 mL of Et$_2$O. This reaction mixture was allowed to react at room temperature for 1 h. Bubbles evolved immediately, and the reaction mixture changed from red to green to brown. All volatiles were removed in vacuo, and the remainder was taken up in Et$_2$O and passed through Celite. This brown solution was concentrated and allowed to crystallize at −35 °C to afford brown crystals in 49% yield based on moles of Ni (0.159 g, 0.245 mmol; max yield = 50%) suitable for single-crystal X-ray analysis.

[Me$_3$NN]Ni(η^2-CH(Ph)NHAd) (4). [Me$_3$NN]Ni═NAd (**1**) (0.375 g, 0.693 mmol) was dissolved in 8 mL of toluene and allowed to stir at room temperature for 72 h. All volatiles were removed in vacuo, and the remaining solid was taken up in 10 mL of Et$_2$O and all volatiles were removed in vacuo again. The remaining solid was taken up in Et$_2$O again and passed through Celite, concentrated, and allowed to crystallize at −35 °C to afford brown crystals in 38% yield based on moles of Ni (0.165 g, 0.261 mmol; max yield = 50%) suitable for single-crystal X-ray analysis. Partial assignment of ^{1}H NMR (C$_6$D$_6$, 400 MHz, room temperature): δ 7.15−6.70 (m, Ar−H), 6.57 (s, 2H, *m*-Ar−H), 5.03 (s, 1H, backbone C−*H*), 2.96 (s, 3H, *p*−Ar−CH$_3$), 2.92 (s, 3H, *p*-Ar−CH$_3$), 2.42 (s, 3H, *o*-Ar−CH$_3$), 2.27 (s, 3H, *o*-Ar−CH$_3$), 2.16 (s, 3H, *o*-Ar−CH$_3$), 1.98 (d, 1H, C*H*Ph or N*H*Ad), 1.81 (d, 1H, C*H*Ph or N*H*Ad), 1.59 (s, 3H, *o*-Ar−CH$_3$ or backbone-CH$_3$), 1.55 (s, 3H, *o*-Ar−CH$_3$ or backbone-CH$_3$), 1.47 (s, 3H, *o*-Ar−CH$_3$ or backbone-CH$_3$), 1.35−1.22 (m, 9H, Ad−H), 0.87 (m, 6H, Ad−H). Despite repeated attempts, we were unable to obtain satisfactory (±0.4%) elemental analysis on this substance.

{[Me$_3$NN]Ni}$_2$(μ-NAd) (5). To a chilled solution of [Me$_3$NN]Ni(2-pic) (0.107 g, 0.234 mmol) in 4 mL of Et$_2$O was added a chilled solution of 1-azidoadamantane (0.021 g, 0.117 mmol) in 2 mL of Et$_2$O. The reaction mixture immediately changed color from red to brown. All volatiles were immediately removed in vacuo. The remaining solid was taken back up in 5 mL of pentane, and all volatiles were immediately removed in vacuo again. The remaining solid was taken up in Et$_2$O passed through Celite, concentrated, and layered with pentane to afford brown crystals in 78% yield (0.085 g, 0.09 mmol) suitable for single-crystal X-ray analysis. ^{1}H NMR (400 MHz, toluene): δ 7.14 (s, 8H, *m*-Ar−H), 2.98 (s, 24H, *o*-Ar−CH$_3$), 2.77 (s, 2H, backbone C−*H*), 2.62 (s, 12H, *p*-Ar−CH$_3$), 1.82 (br, 3H Ad−C*H*), 1.17 (AB q, 6H, Ad−CH$_2$), 0.73 (s, 6H, backbone-CH$_3$), 0.67 (br, 6H, Ad−C*H*$_2$). Anal. Calcd for C$_{56}$H$_{73}$N$_5$Ni$_2$: C, 72.04; H, 7.88; N, 7.50. Found: C, 71.91; H, 7.51; N, 7.18. {[Me$_3$NN]Ni}$_2$(μ-NAd) (**5**) may also be prepared from [Me$_3$NN]Ni═NAd and indane; [Me$_3$NN]Ni═NAd (**1**) (0.375 g, 0.693 mmol) was dissolved in 8 mL of indane. The reaction mixture was allowed to stir at room temperature for 24 h during which a color change from green to brown occurred. All volatiles were removed in vacuo by adding toluene. The remaining solid was taken up in Et$_2$O, filtered through Celite, and concentrated to afford brown crystals in 52% yield (0.157 g, 0.179 mmol).

Computational Details. Most computations employed the Gaussian 09 package.[33] Complete chemical models were studied via the utilization of hybrid ONIOM[34] techniques. The backbone substituents on the β-diketiminate ligand (methyl and mesityl) were modeled with the Universal Force Field (UFF)[35] and the 1-adamantyl substituent (with the exception of the α-carbon). The remainder of the system, including the entire organic substrate, was modeled at the B3LYP/6-311++G(d,p) level of theory. ONIOM(BP86/6-311+G-

(d):UFF) was used to model copper complexes on the basis of its previous use in previously published computational studies of [Cl$_2$NN]Cu═NAd[11] and [Cl$_2$NN]Cu−NHAd.[32] Stationary points were optimized without symmetry constraint, using restricted and unrestricted Kohn−Sham formalisms for closed- and open-shell molecules, respectively. All reported enthalpies and free energies are evaluated using unscaled vibrational frequencies determined at the ONIOM(DFT:UFF) level of theory. All stationary points are characterized as minima (no imaginary frequencies) or transition states (one and only one imaginary frequency) via calculation of the energy Hessian.

Spin density plots for [Me$_3$NN]Ni═NAd (**1**) and triplet [Me$_3$NN]Ni−NHAd (**2-S=1**) in Figure 3 were rendered in ADF[36] by first performing a single point calculation (ADF 2007.1 BP/ZORA/TZ2P(+)) on the optimized coordinates obtained as detailed above. Slater-type orbital (STO) basis sets employed for H, C, and N atoms were of triple-ζ quality augmented with two polarization functions (ZORA/TZ2P), while an improved triple-ζ basis set with two polarization functions (ZORA/TZ2P+) was employed for the Ni atom. Scalar relativistic effects were included by virtue of the zero-order regular approximation (ZORA). The 1s electrons of C and N as well as the 1s−2p electrons of Ni were treated as frozen core.

■ ASSOCIATED CONTENT

Ⓢ Supporting Information
Complete synthetic and kinetics details, additional characterization data for compounds **3**−**5** including EPR spectra, computational methods, X-ray details with fully labeled thermal ellipsoid plots for **3**−**5** (also provided in .cif format), as well as the complete ref 33. This material is available free of charge via the Internet at http://pubs.acs.org.

■ AUTHOR INFORMATION

Corresponding Author
thw@georgetown.edu; t@unt.edu
Notes
The authors declare no competing financial interest.

■ ACKNOWLEDGMENTS

■ REFERENCES

(1) Berry, J. F. *Comments Inorg. Chem.* **2009**, *30*, 28−66.
(2) (a) Dauban, P.; Dodd, R. H. In *Amino Group Chemistry*; Ricci, A., Ed.; Wiley-VCH: Weinheim, 2008; pp 55−92. (b) Collet, F.; Dodd, R. H.; Dauban, P. *Chem. Commun.* **2009**, 5061−5074. (c) Collet, F.; Lescot, C.; Liang, C.; Dauban, P. *Dalton Trans.* **2010**, *39*, 10401−10413. (d) Zalatan, D. N.; Du Bois, J. *Top. Curr. Chem.* **2010**, *292*, 347−378.
(3) (a) Fiori, K. W.; Du Bois, J. *J. Am. Chem. Soc.* **2007**, *129*, 562−568. (b) Liang, C.; Collet, F.; Robert-Peillard, F.; Muller, P.; Dodd, R. H.; Dauban, P. *J. Am. Chem. Soc.* **2008**, *130*, 343−350. (c) Huard, K.; Lebel, H. *Chem.-Eur. J.* **2008**, *14*, 6222−6230. (d) Lebel, H.; Huard, K.; Lectard, S. *J. Am. Chem. Soc.* **2005**, *127*, 14198−14199. (e) Du Bois, J. *Org. Process Res. Dev.* **2011**, *15*, 758−762.
(4) (a) Au, S.-M.; Huang, J.-S.; Yu, W.-Y.; Fung, W.-H.; Che, C.-M. *J. Am. Chem. Soc.* **1999**, *121*, 9120−9132. (b) Leung, S. K.-Y.; Tsui, W.-M.; Huang, J.-S.; Che, C.-M.; Liang, J.-L.; Zhu, N. *J. Am. Chem. Soc.* **2005**, *127*, 16629−16640.
(5) (a) Au, S.-M.; Huang, J.-S.; Che, C.-M.; Yu, W.-Y. *J. Org. Chem.* **2000**, *65*, 7858−7864. (b) Yu, X.-Q.; Huang, J.-S.; Zhou, X.-G.; Che,

C.-M. *Org. Lett.* **2000**, *2*, 2233−2236. (c) Liang, J.-L.; Yuan, S.-X.; Huang, J.-S.; Yu, W.-Y.; Che, C.-M. *Angew. Chem., Int. Ed.* **2002**, *41*, 3465−3468. (d) Milczek, E.; Boudet, N.; Blakey, S. *Angew. Chem., Int. Ed.* **2008**, *47*, 6825−6828. (e) Harvey, M. E.; Musaev, D. G.; Du Bois, J. *J. Am. Chem. Soc.* **2011**, *133*, 17207−17216.

(6) Zhang, J.; Chan, P. W. H.; Che, C.-M. *Tetrahedron Lett.* **2005**, *46*, 5403−5408.

(7) (a) Wang, Z.; Zhang, Y.; Fu, H.; Jiang, Y.; Zhao, Y. *Org. Lett.* **2008**, *10*, 1863−1866. (b) Liu, Y.; Che, C.-M. *Chem.-Eur. J.* **2010**, *16*, 10494−10501.

(8) King, E. R.; Hennessy, E. T.; Betley, T. A. *J. Am. Chem. Soc.* **2011**, *133*, 4917−4923.

(9) (a) Cenini, S.; Gallo, E.; Penoni, A.; Ragaini, F.; Tollari, S. *Chem. Commun.* **2000**, 2265−2266. (b) Caselli, A.; Gallo, E.; Fantauzzi, S.; Morlacchi, S.; Ragaini, F.; Cenini, S. *Eur. J. Inorg. Chem.* **2008**, 3009−3019. (c) Ruppel, J. V.; Kamble, R. M.; Zhang, X. P. *Org. Lett.* **2007**, *9*, 4889−4892. (d) Lu, H.; Tao, J.; Jones, J. E.; Wojitas, L.; Zhang, X. P. *Org. Lett.* **2010**, *12*, 1248−1251. (e) Lu, H.; Subbarayan, V.; Tao, J.; Zhang, X. P. *Organometallics* **2010**, *29*, 389−393. (f) Lyaskovskyy, V.; Olivos Suarez, A. I.; Lu, H.; Jiang, H.; Zhang, X. P.; de Bruin, B. *J. Am. Chem. Soc.* **2011**, *2011*, 12264−12273.

(10) (a) Vedernikov, A. N.; Caulton, K. G. *Chem. Commun.* **2004**, 162−163. (b) Hamilton, C. W.; Laitar, D. S.; Sadighi, J. P. *Chem. Commun.* **2004**, 1628−1629. (c) Díaz-Requejo, M. M.; Belderraín, T. R.; Nicasio, M. C.; Trofimenko, S.; Pérez, P. J. *J. Am. Chem. Soc.* **2003**, *125*, 12078−12079. (d) Fructos, M. R.; Trofimenko, S.; Días-Requejo, M. M.; Pérez, P. J. *J. Am. Chem. Soc.* **2006**, *128*, 11784−11791. (e) Liu, X.; Zhang, Y.; Wang, L.; Fu, H.; Jiang, Y.; Zhao, Y. *J. Org. Chem.* **2008**, *73*, 6207−6212.

(11) Badiei, Y. M.; Dinescu, A.; Dai, X.; Palomino, R. M.; Heinemann, F. W.; Cundari, T. R.; Warren, T. H. *Angew. Chem., Int. Ed.* **2008**, *47*, 9961−9964.

(12) Fantauzzi, S.; Gallo, E.; Caselli, A.; Ragaini, F.; Casati, N.; Macchi, P.; Cenini, S. *Chem. Commun.* **2009**, 3952−3954.

(13) Mindiola, D. J.; Hillhouse, G. L. *J. Am. Chem. Soc.* **2001**, *123*, 4623−4624.

(14) Mindiola, D. J.; Hillhouse, G. L. *Chem. Commun.* **2002**, 1840−1841.

(15) Waterman, R.; Hillhouse, G. L. *J. Am. Chem. Soc.* **2003**, *125*, 13350−13351.

(16) Waterman, R.; Hillhouse, G. L. *J. Am. Chem. Soc.* **2008**, *130*, 12628−12629.

(17) Iluc, V. M.; Miller, A. J. M.; Anderson, J. S.; Monreal, M. J.; Mehn, M. P.; Hillhouse, G. L. *J. Am. Chem. Soc.* **2011**, *133*, 13055−13063.

(18) Laskowski, C. A.; Hillhouse, G. L. *Organometallics* **2009**, *28*, 6114−6120.

(19) Laskowski, C. A.; Miller, A. J. M.; Hillhouse, G. L.; Cundari, T. R. *J. Am. Chem. Soc.* **2011**, *133*, 771−773.

(20) Kogut, E.; Wiencko, H. L.; Zhang, L.; Cordeau, D. E.; Warren, T. H. *J. Am. Chem. Soc.* **2005**, *127*, 11248−11249.

(21) Luo, Y.-R. *Handbook of Bond Dissociation Energies in Organic Compounds*; CRC Press: Boca Raton, FL, 2002.

(22) Bai, G.; Stephan, D. W. *Angew. Chem., Int. Ed.* **2007**, *46*, 1856−1859.

(23) (a) Eckert, N. A.; Vaddadi, S.; Stoian, S.; Lachicotte, R. J.; Cundari, T. R.; Holland, P. L. *Angew. Chem., Int. Ed.* **2006**, *45*, 6868−6871. (b) Cowley, R. E.; Eckert, N. A.; Vaddadi, S.; Figg, T. M.; Cundari, T. R.; Holland, P. L. *J. Am. Chem. Soc.* **2011**, *133*, 9796−9811. (c) Mankad, N. P.; Muller, P.; Peters, J. C. *J. Am. Chem. Soc.* **2010**, *132*, 4083−4085. (d) Nieto, I.; Ding, F.; Bontchev, R. P.; Wang, H.; Smith, J. M. *J. Am. Chem. Soc.* **2008**, *130*, 2716−2717.

(24) Thyagarajan, S.; Shay, D. T.; Incarvito, C. D.; Rheingold, A. L.; Theopold, K. H. *J. Am. Chem. Soc.* **2003**, *125*, 4440−4441.

(25) Iluc, V. M.; Hillhouse, G. L. *J. Am. Chem. Soc.* **2010**, *132*, 15148−15150.

(26) Shay, D. T.; Yap, G. P. A.; Zakharov, L. N.; Rheingold, A. L.; Theopold, K. H. *Angew. Chem., Int. Ed.* **2005**, *44*, 1508−1510.

(27) Cundari, T. R.; Jimenez-Halla, O. C.; Morello, G. R.; Vaddadi, S. *J. Am. Chem. Soc.* **2008**, *130*, 13051−13058.

(28) (a) Pierpont, A. W.; Cundari, T. R. *Inorg. Chem.* **2009**, *48*, 2038−2046. (b) Tekarli, S. M.; Williams, T. G.; Cundari, T. R. *J. Chem. Theory Comput.* **2009**, *5*, 2959−2966.

(29) Badiei, Y. M.; Krishnaswamy, A.; Melzer, M. M.; Warren, T. H. *J. Am. Chem. Soc.* **2006**, *128*, 15056−15057.

(30) Kogut, E.; Zeller, A.; Warren, T. H.; Strassner, T. *J. Am. Chem. Soc.* **2004**, *126*, 11984−11994.

(31) We are grateful to a reviewer for pointing out the importance of steric considerations in the addition of $R^{\bullet}$ to [Ni]=NAd versus [Ni]−NHAd.

(32) Wiese, S.; Badiei, Y. M.; Gephart, R. T.; Mossin, S.; Varonka, M. S.; Melzer, M. M.; Meyer, K.; Cundari, T. R.; Warren, T. H. *Angew. Chem., Int. Ed.* **2010**, *49*, 8850−8855.

(33) Frisch, M. J.; et al. *Gaussian 09*, revision A.1; Gaussian, Inc.: Wallingford, CT, 2009. The complete reference may be found in the Supporting Information.

(34) Dapprich, S.; Komáromi, I.; Byun, K. S.; Morokuma, K.; Frish, M. J. *J. Mol. Struct. (THEOCHEM)* **1999**, *461*, 1−21.

(35) Rappé, A. K.; Casewit, C. J.; Colwell, K. S.; Goddard, W. A. I.; Skiff, W. M. *J. Am. Chem. Soc.* **1992**, *114*, 10024−10035.

(36) (a) te Velde, G.; Bickelhaupt, F. M.; Baerends, E. J.; Fonseca Geurra, C.; Snijders, J. G.; Ziegler, T. *J. Comput. Chem.* **2001**, *22*, 931−967. (b) Fonseca Geurra, C.; Snijders, J. G.; te Velde, G.; Baerends, E. J. *Theor. Chem. Acc.* **1998**, *99*, 391−403.